Structural Safety 70 (2018) 104–114

Contents lists available at ScienceDirect

Structural Safety

journal homepage: www.elsevier.com/locate/strusafe

Non-Gaussian parameter estimation using generalized polynomial chaos expansion with extended Kalman filtering

Subhamoy Sen [a], Baidurya Bhattacharya [b,*]

[a] Indian Institute of Technology Mandi, HP, India
[b] Indian Institute of Technology Kharagpur, WB, India

ARTICLE INFO

Article history:
Received 9 May 2016
Received in revised form 11 October 2017
Accepted 24 October 2017
Available online 2 November 2017

Keywords:
Polynomial chaos expansion
Parameter estimation
Uncertainty quantification
Kalman filer
Extended Kalman filter

ABSTRACT

Kalman Filter (KF) based parameter estimation assumes Gaussianity of the system parameters and thus propagates only the first two moments of the states. Application of Particle filter or Ensemble Kalman filter to estimate non-Gaussian parameters, although more accurate, is computationally expensive. Generalized polynomial chaos (gPC) is well-known as an effective tool to describe any dynamic system with stationary uncertainty through a set of orthogonal basis functions and associated coefficients. This article couples gPC with Extended KF (EKF) algorithm in which the uncertainty propagation from parameter to measurement is described through gPC expansion of parameters and outputs. Subsequently, the gPC coefficients of the parameter expansion are estimated from available measurements employing EKF. Thus, instead of selecting the system parameters as states, we consider the associated parameter gPC coefficients as state variables which reduces the problem of estimating the complete distribution of parameters down to identification of a few gPC coefficients. The proposed method is tested on systems with either Gaussian or non-Gaussian parameters. The error in estimating non-Gaussian parameters using KF based techniques is demonstrated.

1. Introduction

Response prediction of a complex structural system is generally achieved through an idealized mathematical model based initially on a set of prior assumptions and then updated periodically with new information obtained through measurements. The initial idealization and subsequent updating impart uncertainty in the model and its predictions. To enhance the predictive ability of the model, systematic calibration through inverse estimation of parameters from the real measurements is often practised. Commonly, uncertainties in the model parameters are dealt with in a probabilistic framework where variability in the measurement space is mapped back to the parameter space. These types of problems can be categorised under the broad class of stochastic inverse problems.

Direct identification of parameter uncertainty from output variability information requires the simulator model to be invertible, which is not always assured. To reduce computational complexity and time, approximating the actual simulator model by a meta model can be used. Unfortunately, replacing a detailed phenomenological model with a much simplified meta model increases the model uncertainty.

1.1. Existing methods

Identification of parametric uncertainty in probabilistic framework can be performed using Bayesian inference through maximum likelihood estimation (MLE) [1–4]. In MLE approach, the Bayesian estimation problem is posed as a large dimensional optimization problem and subsequently solved using gradient based [5] or other optimization techniques [6,7]. However, due to the non convex nature of this high dimensional problem, obtaining a practical solution often poses as the major challenge.

Kalman filtering [8] (KF) based stochastic data assimilation techniques have been applied extensively to identify system parameter uncertainty from noisy output measurements [9–13] by considering the parameters as additional Gaussian states. KF attempts Bayesian belief propagation to optimally estimate the system states by combining prior belief on states with its likelihood with new measurement. Being a linear estimator, application of KF is limited only to linear systems. This shortcoming led to the introduction of the nonlinear variants of KF (e.g. Extended KF (EKF) [14,15], Unscented KF (UKF) [16] etc.) to handle nonlinear problems by either locally linearising the system or imposing Gaussianity on the posterior distribution. EKF performs first order Taylor series expansion of the state transition functions, while UKF propagates the uncertainty through a set of weighted sigma points

* Corresponding author.
E-mail address: baidurya@civil.iitkgp.ernet.in (B. Bhattacharya).

https://doi.org/10.1016/j.strusafe.2017.10.009
0167-4730/

around the current state estimate. To employ EKF/UKF for parameter estimation, parameters are appended in an extended state vector while representing the otherwise linear system through a bi-linear/nonlinear state space representation [17]. Nevertheless, the assumption on Gaussianity in states or parameters might not always agree with the real situation. Forcibly fitting a Gaussian distribution to a non-Gaussian parameter, in fact, can produce large errors in its estimation.

To accommodate non-Gaussian distributions, particle filter (PF) approaches propagate higher order moments through a set of particles [18–21] and subsequently the posterior estimate is obtained by updating the prior estimate of the particles with their respective likelihood with the current measurement. PF assumes that the parameter domain is discrete and thus updating the prior probability of a discrete set of sample particles using their likelihood gives a measure of the uncertainty in the predefined parameter set. However, with increased dimensionality in the parameter space, the computational demand increases heavily which can render PF computationally inefficient [22]. Apart from these filtering techniques, crude Monte-Carlo sampling based Ensemble Kalman filtering technique offers a robust approach to identifying the parametric variability [23]. However, estimating the probability distribution for the entire set of parameters accurately can be quite expensive.

1.2. Generalized polynomial chaos expansion (gPC)

Introduced by Spanos and Ghanem [24] using the concepts given by Wiener [25] as homogeneous chaos expansion, Polynomial chaos expansion (PCE) technique has emerged as an efficient tool to describe systems with stationary uncertainty using a set of orthogonal bases and associated coefficients [26,27]. PCE can be considered as an advancement of Karhunen–Loeve(KL) expansion [28,29] to discretize any random quantity and to describe its uncertainty through parametrization since the former does not demand the covariance function of the random space to be known a priori. Xiu and Karniadakis [30] later generalized PCE (denoted as gPC) using the result of Cameron-Martin [31] to discretize arbitrary random spaces using hypergeometric orthogonal polynomials chosen from the so called Askey scheme.

In gPC, the physical random variable χ is expressed in terms of a random vector ξ, termed as germ. Based on the selection of germ distribution, a set of mutually orthogonal basis functions (polynomials) $\phi(\xi)$ can be selected. With this germ ξ and polynomial bases $\phi(\xi)$, the physical random variable χ is described as:

$$\chi(\xi) = a_0\phi_0(\xi_0) + \sum_{i_1=1}^{\infty} a_{i_1}\phi_{i_1}(\xi_{i_1}) + \sum_{i_1=1}^{\infty}\sum_{i_2=1}^{\infty} a_{i_1,i_2}\phi_{i_1,i_2}(\xi_{i_1},\xi_{i_2}) + \cdots\infty = \sum_{i=1}^{\infty} a_i\phi_i(\xi) \tag{1}$$

where a_is are the coefficients of the polynomial expansion.

Verlaan and Heemink [32] used the intrusive Galerkin projection approach to solve the coefficients a_i of the expansion. In later works, collocation technique [33] introduced a more efficient approach for estimating the polynomial coefficients.

The basis polynomials vary depending on the germ distribution. For example, for a normally distributed germ, Hermite polynomials are the best suited basis functions, for uniformly distributed germ the basis should be Legendre type and so on. Details of other polynomial basis for different germ distributions are listed in Table 1. To describe a random variable exactly through gPC, an infinite order expansion is ideally required. However, for the sake of practicality, the expansion is generally truncated beyond a certain order.

gPC has been employed by Xiu and Karniadakis [34–36] for solving stochastic differential equations of fluid mechanics problems. Sandu et al. [37–39] employed the gPC technique for multibody dynamics and parameter estimation problems [40]. Soize and Ghanem [41] demonstrated it for estimating arbitrary probability densities. Desceliers et al. [42] employed maximum likelihood estimate (MLE) to identify the gPC coefficients of an arbitrary random filed.

Table 1
Polynomial types for different germ distributions.

Germ distribution	Support domain	Polynomial type
Normal $N(0,1)$	$\mathbb{R}$	Hermite
Uniform $u(-1,1)$	$[-1,1]$	Legendre
Gamma	$\mathbb{R}^+$	Laguerre
Beta	$\mathbb{R}^+$	Jacobi

Pence et al. [54], Pence [55] employed a combination of gPC and MLE in which each point estimate on the probable solution grid is propagated though the system dynamic model using gPC and subsequently MLE is employed to identify the estimate. Jacquelin et al. [56] proposed a modification in gPC to accelerate its convergence. gPC theory has also been extensively used in the literature for uncertainty propagation of otherwise deterministic systems [25,30,43]. This technique is capable of describing an arbitrary parameter distribution in an inexpensive way. It has been extensively used in the context of structural mechanics problems as well [44–48,59–61]. A review of its application for structural vibration problems can be found in Schuëller and Pradlwarter [49]. Sepahvand et al. [50,51] employed gPC for the purpose of parametric uncertainty quantification of stochastic systems. Blanchard et al. [40,52] used gPC technique along with EKF algorithm for parameter identification: gPC solves the forward dynamic state-space problem while EKF updates the state estimates. Li and Xiu [53] demonstrated the application of Ensemble Kalman filtering (EnKF) with gPC theory: the computational efficiency and accuracy are increased by solving the state prediction equation through gPC.

In this article, we couple gPC with Extended Kalman Filter (EKF), to propose a new algorithm in which the uncertainty propagation from parameter to measurement is described using a gPC meta model. The required gPC coefficients of the parameter gPC model are then estimated inversely using EKF. As we show in the following, such an approach enables an accurate and efficient estimation of any random parameter.

2. A new parameter estimation approach

2.1. The problem formulation

Let the system be characterized by a set of parameters $\mathbf{x}$ that are random in nature. There is a map $\mathbb{F}$ (possibly unknown but accurate models of which are available) that relates $\mathbf{x}$ to the system output $\mathbf{y}$. The actual output $\mathbf{y}$ is not known, but can be measured as $\bar{\mathbf{y}}$ repeatedly, giving the collection $\overline{\mathbf{Y}}$. The objective of this study is to determine the probability distribution of $\mathbf{x}$ using the information stored in $\overline{\mathbf{Y}}$ and the best available model $\mathbb{F}$. Algorithm 1 displays the pseudo-code of the coupled gPC-EKF estimator developed in this work.

$\mathbb{F}$ is typically a finite element model that maps each realization in parameter space $\mathbf{x}$ to a corresponding point in output space $\mathbf{y}$. Thus for any parameter-output pair, if the uncertain parameter can be described by a gPC expansion with a set of germs as its argument, the associated output gPC expansion can always be defined by the same set of germs:

$$\mathbf{y}(\underline{\xi}) = \mathbb{F}(\mathbf{x}(\underline{\xi})) \tag{2}$$

where $\mathbf{x}(\underline{\xi}) = [x_1(\xi_1), x_2(\xi_2), \ldots, x_n(\xi_n)]$ is the parameter vector and $\underline{\xi} = [\xi_1, \xi_2, \ldots, \xi_n]$ is the associated germ vector.

$\mathbf{y}(\underline{\xi}) = [y_1(\underline{\xi}), y_2(\underline{\xi}), \ldots, y_m(\underline{\xi})]$ are the outputs defined by the same set of germs $\underline{\xi}$.

The truncated gPC expansion for the k^{th} input and the k^{th} output with j_x and j_y dimensional germs involving up to p_x^{th} and p_y^{th} order terms respectively can be described respectively as:

$$x_k(\xi_k) = \sum_{i=1}^{s_x(p_x,j_x)} a_i^{x_k}\phi_i^{x_k}(\xi_k) = \phi^{x_k}\mathbf{a}^{x_k}; \tag{3a}$$

and

$$y_k(\underline{\xi}) = \mathbb{F}_k(\{x_1(\xi_1), x_2(\xi_2), \ldots, x_n(\xi_n)\}) = \sum_{i=1}^{s_y(p_y,j_y)} a_i^{y_k}\phi_i^{y_k}(\underline{\xi}) = \phi^{y_k}\mathbf{a}^{y_k}; \tag{3b}$$

where $\phi^{x_k} = [\phi_1^{x_k}, \phi_2^{x_k}, \ldots, \phi_{s_x}^{x_k}]$, and $\phi^{y_k} = [\phi_1^{y_k}, \phi_2^{y_k}, \ldots, \phi_{s_y}^{y_k}]$. $\mathbf{a}^{x_k} = [a_1^{x_k}, a_2^{x_k}, \ldots, a_{s_x}^{x_k}]^T$ and $\mathbf{a}^{y_k} = [a_1^{y_k}, a_2^{y_k}, \ldots, a_{s_y}^{y_k}]^T$ are the polynomial coefficients for their respective gPC expansions.

$s_x(p_x,j_x)$ and $s_y(p_y,j_y)$ are the required number of terms in the chaos expansion in order to encompass up to p_x^{th} and p_y^{th} order polynomial for parameters and outputs respectively. For example, for the parameter x_k, the required number of terms (s_x) in gPC expansion can be determined from the chosen order of basis polynomials (p_x) and the number of germ variable (j_x) as:

$$s_x = \frac{(p_x + j_x)!}{p_x! j_x!} \tag{4}$$

The parameters $x_1, x_2, \ldots, x_n$ in this problem are assumed to be independent and thus each is described by a one dimensional gPC using a single germ. The outputs, being functions of all n parameters, are expanded using n dimensional gPC basis expressed as the tensor product of parameter gPC bases:

$$\phi^{y_i}(\underline{\xi}) = \prod_{j=1}^{n}\left(\phi^{x_j}(\xi_j)\right) \quad i = 1,2,\ldots,m \quad \text{and } j = 1,2,\ldots,n. \tag{5}$$

The above discussion intends to demonstrate how the uncertainty in the parameter space propagates to the measurement space and how the associated uncertainties can be described through the same germ vector $\underline{\xi}$ for both parameter and output measurement. For the same set of polynomials $\phi^{x_k}(\xi_k)$ and $\phi^{y_k}(\underline{\xi})$, the distributions of parameters and outputs however differ based on the coefficients $\mathbf{a}^{x_k}$ and $\mathbf{a}^{y_k}$.

2.2. Identification of the output gPC

Let $\underline{\xi}^{(l)} = [\xi_1^{(l)}, \xi_2^{(l)}, \ldots \xi_n^{(l)}]$ be the l^{th} realization of the germ vector $\underline{\xi}$ in which each germ $\xi_k^{(l)}$ is associated with the l^{th} realization of the k^{th} system parameter x_k:

$$x_k^{(l)}(\xi_k^{(l)}) = \sum_{i=1}^{s_x(p_x,j_x)} a_i^{x_k}\phi_i^{x_k}(\xi_k^{(l)}); k = 1,2,\ldots n; \text{ and } \quad l = 1,2,\ldots N \tag{6}$$

Thus the output realization $y_k^{(l)}$ associated to this particular parameter set $[x_1^{(l)}, x_2^{(l)}, \ldots, x_n^{(l)}]$ will obviously be a function of the germ set $\underline{\xi}^{(l)}$.

As stated above, the actual output ($\mathbf{y}$) is unknown but can be observed through measurements $\bar{\mathbf{y}}$ collected from the system. $\overline{\mathbf{Y}}$ is an array of N such measurements. These N such output realizations are associated to N different germ sets as: $\{\Xi\} = [\underline{\xi}^{(1)}, \underline{\xi}^{(2)}, \ldots, \underline{\xi}^{(l)}, \ldots, \underline{\xi}^{(N)}]^T$. Since the measured outputs $\overline{\mathbf{Y}}$ are known, a gPC model for $\mathbf{y}$ can always be fitted to the data, say, using Galerkin projection technique. This fitted model $\widetilde{\mathbf{y}}(\underline{\xi})$ has the structure of $\widetilde{\mathbf{y}}(\underline{\xi}) = \phi_y(\underline{\xi})\widetilde{\mathbf{a}}^y$ with the germ $(\underline{\xi})$ being its argument through which the associated uncertainty is defined. This fitted model can subsequently be used to generate a large number of realizations of the synthetic output $\widetilde{\mathbf{Y}}$ in a computationally inexpensive way. This, in turn, provides a measurement model required for the EKF algorithm.

The required coefficients $\widetilde{\mathbf{a}}^y$ for the gPC model $\widetilde{\mathbf{y}}(\underline{\xi})$ of the actual output variable $\mathbf{y}$ is obtained using Galerkin projection technique as (Step 6 and 7 of Algo. 1):

$$\tilde{a}_j^{y_k} = \frac{\sum_{i=1}^{N} y_k^{(i)}\phi_j^y(\underline{\xi}^{(i)})}{\sum_{i=1}^{N}\phi_j^y(\underline{\xi}^{(i)})\phi_j^y(\underline{\xi}^{(i)})}; \quad \text{for} \quad k = 1,2,\ldots,m \tag{7}$$

This fitted gPC model can then be used to simulate output realizations $\widetilde{\mathbf{Y}}$ as $\widetilde{\mathbf{Y}} = \phi^{y_k}(\underline{\xi})\widetilde{\mathbf{a}}^{y_k}$ for different realizations of $\underline{\xi}$. Although not essential, this step yields stable estimates of higher moments of the response which are required in the inverse EKF estimation. The alternative of using moments directly computed from the raw data can give rise to convergence issues.

The l^{th} realization of the k^{th} output is then given by the following gPC expansion involving all n germs associated with the n system parameters (cf. Eq. (2)):

$$y_k^{(l)}(\underline{\xi}^{(l)}) = \sum_{i=1}^{s_y(p_y,j_y)} a_i^{y_k}\phi_i^{y_k}(\underline{\xi}^{(l)}); k = 1,2,\ldots m; \quad \text{and} \quad l = 1,2,\ldots N \tag{8}$$

In this study, all outputs are defined using the same set of polynomial bases, i.e. $\phi^{y_1}(\underline{\xi}) = \phi^{y_2}(\underline{\xi}) = \cdots = \phi^{y_m}(\underline{\xi}) = \phi^{y}(\underline{\xi})$. The multivariate gPC expansion for N sets of output realizations can then be expanded as:

$$\begin{bmatrix} \phi_1^y(\underline{\xi}^{(1)}) & \phi_2^y(\underline{\xi}^{(1)}) & \cdots & \phi_{s_y}^y(\underline{\xi}^{(1)}) \\ \phi_1^y(\underline{\xi}^{(2)}) & \phi_2^y(\underline{\xi}^{(2)}) & \cdots & \phi_{s_y}^y(\underline{\xi}^{(2)}) \\ \phi_1^y(\underline{\xi}^{(3)}) & \phi_2^y(\underline{\xi}^{(3)}) & \cdots & \phi_{s_y}^y(\underline{\xi}^{(3)}) \\ \vdots & \vdots & \ddots & \vdots \\ \phi_1^y(\underline{\xi}^{(N)}) & \phi_2^y(\underline{\xi}^{(N)}) & \cdots & \phi_{s_y}^y(\underline{\xi}^{(N)}) \end{bmatrix} \begin{bmatrix} a_1^{y_1} & a_1^{y_2} & \cdots & a_1^{y_m} \\ a_2^{y_1} & a_2^{y_2} & \cdots & a_2^{y_m} \\ a_3^{y_1} & a_3^{y_2} & \cdots & a_3^{y_m} \\ \vdots & \vdots & \ddots & \vdots \\ a_{s_y}^{y_1} & a_{s_y}^{y_2} & \cdots & a_{s_y}^{y_m} \end{bmatrix} = \begin{bmatrix} y_1^{(1)} & y_2^{(1)} & \cdots & y_m^{(1)} \\ y_1^{(2)} & y_2^{(2)} & \cdots & y_m^{(2)} \\ y_1^{(3)} & y_2^{(3)} & \cdots & y_m^{(3)} \\ \vdots & \vdots & \ddots & \vdots \\ y_1^{(N)} & y_2^{(N)} & \cdots & y_m^{(N)} \end{bmatrix} \tag{9}$$

In order to obtain a gPC model for the outputs, the polynomials can be assumed based on the germ type which in turn depends on the distribution type (cf. Table 1). However, it is often expensive to collect measured output data $\overline{\mathbf{Y}}$ which makes the accurate classification of the output distribution a challenge. Pearson's model criteria [57,58] offers a good solution in this context (c.f. Appendix A). This method identifies the underlying approximate distribution from the limited available data. This in turn helps in selecting the appropriate germ distribution for the output gPC expansion (Steps 1 and 2 of Algo. 1). Selection of proper germ type helps in reducing computational complexity since with the proper germ, the random varible can be defined with least amount of expansion terms in the truncated expansion [54].

2.3. EKF based estimation of the parameter gPC coefficients

Unlike the outputs, the system parameters $\mathbf{x}$ are not directly observable and thus one cannot develop a fitted gPC model for parameters directly. However, these parameters are related to the corresponding measurements through the map $\mathbb{F}$ (cf. Eq. (2)). This study expresses each system parameter through a gPC model (Eq. (3a)) with a set of assumed gPC polynomials and initial guess for the gPC coefficients $\{\mathbf{a}^{x_1}, \mathbf{a}^{x_2}, \ldots \mathbf{a}^{x_n}\}$. These parameter gPC coefficients are then considered as unobservable system states observed through the measured output $\mathbf{Y}$ (or its fitted model $\widetilde{\mathbf{y}}(\underline{\xi})$ if necessary). EKF is then employed to estimate the coefficients as states optimally by minimizing the error covariances in state estimates.

EKF estimates an optimal set of gPC coefficients $\widehat{\mathbf{a}}^{\mathbf{x}} = [\widehat{\mathbf{a}}^{x_1}, \widehat{\mathbf{a}}^{x_2}, \ldots, \widehat{\mathbf{a}}^{x_n}]$ for which the estimated output moments optimally match those of the actually measured or synthetically generated output (Since the proposed method is numerically validated in this article, the expressions the "actually measured output" and "synthetically generated output" are synonymous here.). Moments of the measured output are thus considered as observations in this estimation. EKF recursively updates the prior estimate of $\widehat{\mathbf{a}}^{\mathbf{x}}$ by mapping the mismatch between moments associated with the current estimate $\widehat{\mathbf{a}}^{\mathbf{x}}$ and the actual moments (i.e. innovation) back to the parameter space using a suitable gain matrix $\mathbf{K}$. $\mathbf{K}$ incorporates the feedback as correction in the current estimate $\widehat{\mathbf{a}}^{\mathbf{x}}$. The optimal solution thus asymptotically converges to an estimate for which the error between actual and estimated moments minimizes.

EKF considers gPC coefficients $\widehat{\mathbf{a}}^{\mathbf{x}}_{t|t}$ as system states with its dynamics defined in pseudo-time t as:

$$\text{Process equation}: \quad \widehat{\mathbf{a}}^{\mathbf{x}}_{t|t-1} = \widehat{\mathbf{a}}^{\mathbf{x}}_{t-1|t-1} + \mathbf{v}_t; \tag{10}$$

After each time update, the propagated estimate $\widehat{\mathbf{a}}^{\mathbf{x}}_{t|t-1}$ is observed through output moments. The measurement equation measures the error in the state estimate thorugh the error between the estimated and actual moments of the outputs as:

$$\text{Measurement equation}: \quad \epsilon_t = \{\mathbf{M}_{\mathbf{Y}} - \mathbb{M}(\widehat{\mathbf{a}}^{\mathbf{x}}_{t|t-1})\} + \mathbf{w}_t; \tag{11}$$

$\mathbf{v}_t$ and $\mathbf{w}_t$ are the process and measurement noise modeled as Gaussian white noise with covariances $\mathbf{Q}$ and $\mathbf{R}$ respectively. $\mathbb{M}(\bullet)$ is a mapping of the parameter gPC coefficients $\widehat{\mathbf{a}}^{\mathbf{x}}_{t|t-1}$ to the moments of the corresponding outputs and $\mathbf{M}_{\mathbf{Y}}$ is the actual moment obtained either directly from the measured output $\overline{\mathbf{Y}}$ or its fitted model $\widetilde{\mathbf{Y}}$. The notation $\widehat{\mathbf{a}}^{\mathbf{x}}_{t_1|t_2}$ signifies an estimate of $\mathbf{a}^{\mathbf{x}}$ at t_1^{th} instant incorporating information up to t_2^{th} instant.

ϵ_t, the difference between the moments of actual and estimated outpout, is considered as the measurement innovation. In this article, the error measure ϵ_t (as defined in Eq. (11)) is considered to be the difference between the first four moments of the fitted ($\widetilde{\mathbf{Y}}$) and estimated ($\widehat{\mathbf{Y}}$) outputs. Selection of higher order moements in inovation formulation not only helps match the spread but the tail of the distribution as well [51]. The mismatch along with the Kalman gain is then used to update the current estimate of coefficients recursively (cf. Eq. (12)). The iterations are carried out until a predefined tolerance is achieved.

We should note here that, in order to measure the statistical moments in the estimated output, sufficient output realizations are usually required. This in turn demands expensive FE calls which is not practical. Collocation method is employed in this endeavour to minimize this expensive FE calls.

In each step of EKF, the current state estimate $\widehat{\mathbf{a}}^{\mathbf{x}}_{t|t-1}$ is propagated through the system model for a few selectively chosen germs only (collocation points $\underline{\xi}^c$) and the associated outputs are obtained (Step 9 of Algo. 1). Subsequently, from this parameter-output prediction pair, a gPC model $\widehat{\mathbf{y}}(\underline{\xi})$ with the output gPC coefficients $\widehat{\mathbf{a}}^{y}_{t|t-1}, k = 1, 2, \ldots m$, are obtained (Step 10 of Algo. 1). Monte-Carlo simulations are then performed on this estimated output gPC model, $\widehat{\mathbf{y}}(\underline{\xi})$ for sampling output estimates $\widehat{\mathbf{Y}}$. Eventually, a large set of estimated output realizations $\widehat{\mathbf{Y}}$ can be generated from which the moment estimates associated to $\widehat{\mathbf{a}}^{\mathbf{x}}_{t|t-1}$ are obtained. A similar process is also followed to obtain the moments of the simulated outputs $\widetilde{\mathbf{Y}}$ realized from the fitted model $\widetilde{\mathbf{y}}(\underline{\xi})$ for a germ set of same length.

Subsequently, the measurement correction can be incorporated in the predicted estimate $\widehat{\mathbf{a}}^{\mathbf{x}}_{t|t-1}$ as:

$$\widehat{\mathbf{a}}^{\mathbf{x}}_{t|t} = \widehat{\mathbf{a}}^{\mathbf{x}}_{t|t-1} + \mathbf{K}_t \epsilon_t; \tag{12}$$

where $\mathbf{K}_t$ is the Kalman gain at t^{th} iteration step to incorporate the measurement mismatch ϵ_t as feedback into the corrected state estimate.

Algorithm 1: Coupled gPC-EKF algorithm

Step 1: Identify the Output distribution type and select the appropriate germs and associated polynomial types for output and parameter gPC models from Table 1. Use these one dimensional polynomials to define the multidimensional polynomial for output gPC model.
Step 2: Assume a prior estimate $\widehat{\mathbf{a}}^{\mathbf{x}}_{0|0}$ for the coefficients of the parameter gPC model.
Step 3: Obtain the collocation points for each parameter. (These are the roots of $(p+1)^{th}$ order polynomial where p is the highest order of polynomials considered in expansion.)
Step 4: Simulate a set of germs ($\underline{\xi}^c = \{\underline{\xi}^{(l)}\}$ for $l = 1, 2, \ldots, n_c$) with different combination of the collocation points. n_c is the number of combinations of collocation points.

Obtaining the output gPC coefficients and moments
Step 5: Estimate gPC coefficients $\widetilde{\mathbf{a}}^{y_k}$ for all $k = 1, 2, \ldots, m$ of the fitted gPC model $\widetilde{\mathbf{y}}(\underline{\xi})$ for the measured output $\overline{\mathbf{Y}}$ using Eq. (7).
Step 6: Use the fitted gPC model $\widetilde{\mathbf{y}}(\underline{\xi})$ to simulate output realizations $\widetilde{\mathbf{Y}}$ for different $\underline{\xi}$ values.

Start Extended Kalman filter
Iterations (while error < tolerance)
Prediction step
Step 7: Propagate the mean and covariance of states $\widehat{\mathbf{a}}^{\mathbf{x}}_{t-1|t-1}$ in pseudo time t as:
State prediction: $\widehat{\mathbf{a}}^{\mathbf{x}}_{t|t-1} = \widehat{\mathbf{a}}^{\mathbf{x}}_{t-1|t-1}$;
State covariance prediction: $\mathbf{P}_{t|t-1} = \mathbf{P}_{t-1|t-1} + \mathbf{Q}_t$;

Correction step
Step 8: Using $\widehat{\mathbf{a}}^{\mathbf{x}}_{t|t-1}$, map the collocation germ sets ($\underline{\xi}^c$) to a set of parameters realization $\hat{\mathbf{x}}_t = \{\hat{\mathbf{x}}_t^{(l)}\}$ for $l = 1, 2, \ldots n_c$.
Step 9: Simulate the system model $\mathbb{F}$ (usually the FEM) for each parameter set as: $\hat{\mathbf{y}}_t^{(l)} = \mathbb{F}(\hat{\mathbf{x}}_t^{(l)})$ for $l = 1, 2, \ldots, n_c$. Collect outputs for all l in $\widehat{\mathbf{Y}}_t^c$
Step 10: Fit a gPC model to $\widehat{\mathbf{Y}}_t^c$ using collocation method and estimate corresponding gPC coefficients as $\widehat{\mathbf{a}}^{\mathbf{y}}_{t|t-1}$ (cf. Eq. (7)).
Step 11: Using Eq. (3b) and current estimate for output gPC coefficient $\widehat{\mathbf{a}}^{\mathbf{y}}_{t|t-1}$, simulate a set of output realizations $\widehat{\mathbf{Y}}$.
Step 12: Calculate the error between simulated ($\widetilde{\mathbf{Y}}$) and estimated ($\widehat{\mathbf{Y}}$) output moments: $\epsilon = \mathbf{M}_{\widetilde{\mathbf{Y}}} - \mathbf{M}_{\widehat{\mathbf{Y}}}$, where $\mathbf{M}$ signifies moment.
Step 13: Calculate the innovation covariance: $\mathbf{S}_t = \mathbf{H}_t \mathbf{P}_{t|t-1} \mathbf{H}_t^T + \mathbf{R}_t$; where $\mathbf{H}_t = \nabla_a(\epsilon)|_{\widehat{\mathbf{a}}^{\mathbf{x}}_{t|t-1}}$
Step 14: Calculate the gain matrix $\mathbf{K}_t$: $\mathbf{K}_t = \mathbf{P}_{t|t-1} \mathbf{H}_t^T \mathbf{S}_t^{-1}$
Step 15: Update state estimate: $\widehat{\mathbf{a}}^{\mathbf{x}}_{t|t} = \widehat{\mathbf{a}}^{\mathbf{x}}_{t|t-1} + \mathbf{K}_t \epsilon_t$;
Step 16: Update state covariance: $\mathbf{P}_{t|t} = (\mathbf{I} - \mathbf{K}_t \mathbf{H}_t) \mathbf{P}_{t|t-1}$;
Step 17: Go to Step 8 till tolerance is achieved.

3. Numerical examples

We analyze a 0.45 m × 0.25 m × 0.006 m cantilevered plate supported at its shorter edge. The plate is modelled with 10 × 10 Mindlin-Reissner plate elements and the Finite Element (FE) model is assumed to be sufficiently accurate so that model uncertainty can be ignored. Elasticity ($x_1 = E$) and Poisson's ratio ($x_2 = \nu$) of the plate are considered to be the unknown parameters. Two cases are considered: (i) E and ν are independent Gaussian, and (ii) E and ν are independent and each is Beta distributed. In each case, the plate is subjected to white noise vibration along its free end and acceleration time series are recorded for 10 s at a node 0.05 m X 0.09 m away from one corner of the free end. This signal is subsequently contaminated with 2% Gaussian white noise.

The process is repeated 1000 times in order to eliminate small sample uncertainties and for each experiment the acceleration responses are collected at the measurement point. A Fourier domain decomposition of acceleration time histories to construct the frequency response plot and subsequent peak picking leads to identification of the natural frequencies. The first five natural frequencies, $\{\bar{y}_i, i = 1\ldots,5\}$, are thus obtained as measurements from the time series data. Eventually, thousand such experiments generates an array of measurement data $\overline{\mathbf{Y}}$, (although in a real life scenario, the process can be repeated perhaps only a few hundred times).

In each case, the distributions of E and ν are estimated (a) first with the proposed gPC - EKF method that can estimate any arbitrary distribution, and (b) the traditional EKF and UKF based Gaussian parameter estimation methods. In the first case when the parameters are actually Gaussian, even though EKF and UKF gives sufficiently accurate estimates of the means, the variance estimates significantly deviate from the true values. The problem becomes more prominent in the second case when the parameters are in fact non-Gaussian; the proposed method significantly outperforms the traditional methods, as we describe next.

3.1. Gaussian case

The "true" distributions of the plate parameters (i.e. E and ν) are listed in Table 2. As stated above, the parameters are sampled from their "true" distributions 1000 times, and propagated through the system model $\mathbb{F}$ to yield the measurements $\overline{\mathbf{Y}}$. The measurement distribution, when put through the Pearson classification scheme, is identified as Gaussian. Gaussian random numbers are therefore selected for the germ distribution and associated Hermite polynomials are selected for chaos expansion accordingly.

To select the maximum order of polynomials to be used for the expansion, a separate study is usually undertaken. We have employed five different order polynomials to describe the variability in the output and the evolution of Kullback–Leibler (KL) divergence between actual and estimated distributions of the output against increasing polynomial orders are presented in Fig. 1. It can be verified from the figure that beyond the second order, the precision does not improve much while the computational effort increases. Second order polynomials are therefore considered for the outputs. Selection of the order of polynomial for parameter distribution, however, can not be made a priori. A conservative selection of third order polynomials for both Gaussian and non-Gaussian cases are therefore made, even though, first order polynomial would have been sufficient especially for the Gaussian parameters.

Table 2
"True" distributions of the unknown plate parameters: Gaussian case.

	Elasticity (GPa)	Poisson's ratio (ν)
Distribution	Gaussian	Gaussian
Mean	62.85	0.334
COV (%)	10	10

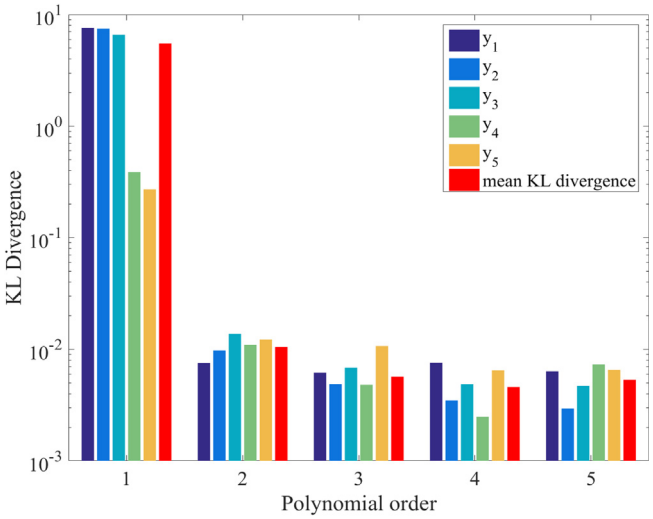

Fig. 1. KL Divergence over increasing order of polynomials.

The expansion is therefore truncated beyond second order of polynomials for the "fitted" output expansion:

$$\begin{aligned}\tilde{y}_i(\underline{\xi}) &= y_i(\{\xi_1, \xi_2\}) \\ &= a_0^{y_i} + a_1^{y_i}\xi_2 + a_2^{\bar{y}_i}\xi_1 + a_3^{y_i}(\xi_2^2 - 1) + a_4^{y_i}\xi_1\xi_2 + a_5^{y_i}(\xi_1^2 - 1) \end{aligned} \quad (13)$$

Thus $\frac{(2+2)!}{2!2!} = 6$ polynomial terms and associated coefficients are required to describe each of the output, which needs to be estimated from the available measurements $\overline{\mathbf{Y}}$. Table 3 lists the identified gPC coefficients for the fitted output. This gPC model of the fitted output is subsequently used to simulate a sufficiently large set $\widetilde{\mathbf{Y}}$. Table 4 compares the first four moments of the measured ($\overline{\mathbf{Y}}$) and fitted outputs ($\widetilde{\mathbf{Y}}$).

Parameter estimation is now taken up using the proposed gPC-EKF method. The same germs used in Eq. (13) are assumed to govern the parameter expansion. The polynomial is truncated beyond the third order:

$$\begin{aligned} x_1(\xi_1) &= a_0^{x_1} + a_1^{x_1}\xi_1 + a_2^{x_1}(\xi_1^2 - 1) + a_3^{x_1}(\xi_1^3 - 3\xi_1); \\ x_2(\xi_2) &= a_0^{x_2} + a_1^{x_2}\xi_2 + a_2^{x_2}(\xi_2^2 - 1) + a_3^{x_2}(\xi_2^3 - 3\xi_2); \end{aligned} \quad (14)$$

Each input is thus defined using $\frac{(3+1)!}{3!1!} = 4$ polynomials terms and their respective coefficients which are estimated as system states.

In each iteration, the current estimate $\widehat{\mathbf{a}}^{\mathbf{x}}_{t|t-1}$ is used to obtain the system parameters $\hat{\mathbf{x}}$ at the collocation points ($\underline{\xi}^c$) (Step 9, Algo. 1) which are subsequently propagated through the system model to get the outputs $\hat{\mathbf{y}}$ (Step 10, Algo. 1). An estimate of the output gPC coefficients $\widehat{\mathbf{a}}^{y}_{t|t-1}$ is then obtained from this output set (Step 10 of Algo. 1). The current estimates of the output gPC coefficient are then employed to simulate output realizations $\widehat{\mathbf{Y}}$ (Step 11, Algo. 1). The mismatch between the first four moments of $\widehat{\mathbf{Y}}$ and $\widetilde{\mathbf{Y}}$ are used to define the error measure ϵ_t (Step 12, Algo. 1). The current estimate of $\widehat{\mathbf{a}}^{\mathbf{x}}_{t|t-1}$ is then corrected using the Kalman gain and ϵ_i(Steps 13–16, Algo. 1) until convergence is reached. Table 5 lists the estimated parameter gPC coefficients thus obtained. Statistical properties and distributions of E and ν can be obtained through Monte Carlo simulation of the respective gPC expansions. The

Table 3
gPC coefficients for the "fitted" output measurement: Gaussian case.

gPC expansion $f(\{\xi_1,\xi_2\}) = a_0^{y_i} + a_1^{y_i}\xi_2 + a_2^{y_i}\xi_1 + a_3^{y_i}(\xi_2^2-1) + a_4^{y_i}\xi_1\xi_2 + a_5^{y_i}(\xi_1^2-1)$						
Coefficients	$a_0^{y_i}$	$a_1^{y_i}$	$a_2^{y_i}$	$a_3^{y_i}$	$a_4^{y_i}$	$a_5^{y_i}$
$\tilde{y}_1$	23.710	−1.130	0.409	0.021	0.102	0.099
$\tilde{y}_2$	90.293	4.531	0.102	−0.116	−0.073	0.540
$\tilde{y}_3$	161.60	−7.807	2.435	0.003	0.076	0.028
$\tilde{y}_4$	319.65	−15.62	3.871	0.040	0.907	0.825
$\tilde{y}_5$	517.51	−24.82	7.300	0.302	2.224	1.858

Table 4
Comparison of moments of measured $\bar{\mathbf{Y}}$ and "fitted" $\tilde{\mathbf{Y}}$ outputs for Gaussian case.

	Mean (Hz)		Std dev. (Hz)		Skewness		Kurtosis	
	Measured	Fitted	Measured	Fitted	Measured	Fitted	Measured	Fitted
y_1	23.653	23.702	1.204	1.250	−0.093	−0.085	3.213	2.986
y_2	90.466	90.563	4.572	4.820	−0.105	0.002	3.001	3.112
y_3	161.26	161.58	8.162	8.491	−0.099	−0.080	3.196	2.999
y_4	319.20	319.61	16.02	16.87	−0.111	−0.019	3.044	3.089
y_5	516.55	517.39	25.88	27.10	−0.111	−0.057	3.133	3.039

Table 5
gPC coefficients for system parameters: Gaussian case.

gPC expansion $x_i(\xi_i) = a_0^{x_i} + a_1^{x_i}\xi_i + a_2^{x_i}(\xi_i^2-1) + a_3^{x_i}(\xi_i^3-3\xi_i)$				
Coefficients	$a_0^{x_i}$	$a_1^{x_i}$	$a_2^{x_i}$	$a_3^{x_i}$
E (x_1) (GPa)	63.29	6.56	0.22	0
ν (x_2)	0.334	0.034	0	0

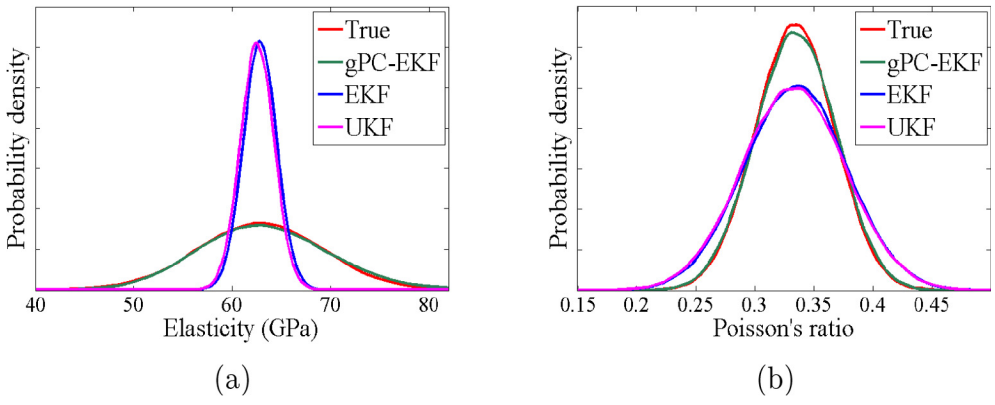

Fig. 2. Performance of proposed gPC-EKF and traditional KF algorithms in identifying "true" densities of system parameters: Gaussian case.

Table 6
Performance of proposed gPC-EKF and traditional KF algorithms in identifying "true" moments of system parameters: Gaussian case. Note that, being linear Gaussian estimators, EKF and UKF are unable to estimate moments higher than the second.

	Mean (GPa)		Std dev. (GPa)		Skewness		Kurtosis	
	"True"	Identified	"True"	Identified	"True"	Identified	"True"	Identified
Elasticity								
gPC-EKF	62.85	63.32	6.29	6.58	0	0.204	3.0	3.054
EKF	62.85	62.84	6.29	1.71	0	–	3.0	–
UKF	62.85	62.55	6.29	1.72	0	–	3.0	–
Poisson's ratio								
gPC-EKF	0.334	0.3345	0.033	0.034	0	−0.041	3.0	2.906
EKF	0.334	0.334	0.033	0.043	0	–	3.0	–
UKF	0.334	0.333	0.033	0.047	0	–	3.0	–

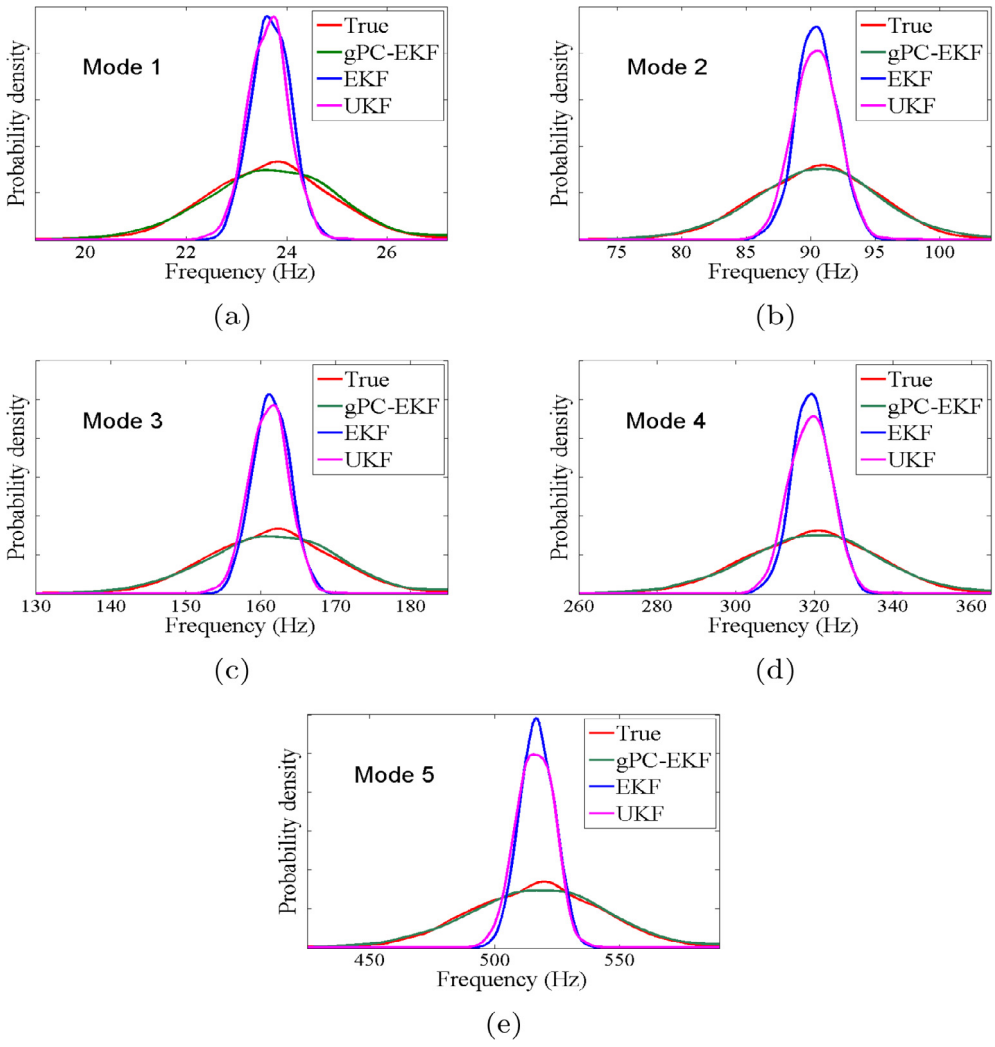

Fig. 3. Performance of proposed gPC-EKF algorithm vis à vis the traditional KF algorithms in reproducing the probability densities of the first five modal frequencies: Gaussian system parameters.

Table 7
"True" distributions of the unknown plate parameters: non Gaussian case.

Elasticity (GPa)		Poisson's ratio (ν)
Distribution	Beta	Beta
Mean	44.95	0.124
Std. dev.	10	0.068
α, β	$\{5, 2.5\}$	$\{2, 11\}$

distribution of the estimated outputs too can be obtained from these same realizations.

Fig. 2a and b compare the density functions of E and ν obtained using the proposed gPC-EKF algorithm with the true densities. Table 6 lists the first four moments of these densities. Fig. 3 compares the measured *vs.* estimated densities of first five natural frequencies of the plate. It is clear that the proposed algorithm is able to accurately identify the distributions of the unknown system parameters.

In order to compare our method with linear estimators, we solve the example using traditional EKF and UKF methods in which the parameters themselves are considered as the system states. Figs. 2a, b and Table 6 show the corresponding results. It is clear that even in this Gaussian case, the traditional KF algorithms fall short: they are able to estimate the mean satisfactorily, but not the higher moments.

Table 8
gPC coefficients for the "fitted" output measurement: non-Gaussian case.

gPC expansion
$y_i(\underline{\xi}) = y_i(\{\xi_1, \xi_2\}) = a_0^{y_i} + a_1^{y_i}\xi_2 + a_2^{y_i}\xi_1 + a_3^{y_i}(\frac{3}{2}\xi_2^2 - \frac{1}{2}) + a_4^{y_i}\xi_1\xi_2 + a_5^{y_i}(\frac{3}{2}\xi_1^2 - \frac{1}{2})$

Coefficients	$a_0^{y_i}$	$a_1^{y_i}$	$a_2^{y_i}$	$a_3^{y_i}$	$a_4^{y_i}$	$a_5^{y_i}$
$\tilde{y}_1$	19.560	2.118	−0.553	−0.413	−0.022	0.215
$\tilde{y}_2$	82.993	−3.080	8.617	−1.303	−0.839	−1.150
$\tilde{y}_3$	135.67	−1.438	15.29	−0.469	0.218	−1.941
$\tilde{y}_4$	283.38	−20.48	−25.13	−1.718	−2.935	−2.980
$\tilde{y}_5$	440.43	44.57	−22.41	−8.040	11.33	4.829

Table 9
Comparison of moments of measured $\overline{\mathbf{Y}}$ and "fitted" $\widetilde{\mathbf{Y}}$ outputs for non Gaussian case study.

	Mean (Hz)		Std dev. (Hz)		Skewness		Kurtosis	
	Measured	Fitted	Measured	Fitted	Measured	Fitted	Measured	Fitted
y_1	19.390	19.390	2.400	2.572	−1.118	−1.416	4.454	6.815
y_2	81.497	80.217	10.06	10.75	−1.095	−1.328	4.453	6.621
y_3	133.14	133.01	16.46	17.61	−1.122	−1.425	4.465	6.844
y_4	282.50	278.89	34.74	37.08	−1.118	−1.376	4.493	6.765
y_5	441.71	438.51	54.23	57.87	−1.140	−1.430	4.520	6.908

Table 10
gPC coefficients for system parameters: non-Gaussian case.

gPC expansion
$x_i(\xi_i) = a_0^{x_i} + a_i^{x_i}\xi_i + a_2^{x_i}(\frac{3}{2}\xi_i^2 - \frac{1}{2}) + a_3^{x_i}(\frac{5}{2}\xi_i^3 - \frac{3}{2}\xi_i)$

Coefficients	$a_0^{x_i}$	$a_1^{x_i}$	$a_2^{x_i}$	$a_3^{x_i}$
E (x_1) (GPa)	44.94	10.55	−1.01	−0.01
ν (x_2)	0.147	0.086	0.009	0

Table 11
Performance of proposed gPC-EKF and traditional KF algorithms in identifying "true" moments of system parameters: non-Gaussian case. Note that, being linear Gaussian estimators, EKF and UKF are unable to estimate moments higher than the second.

	Mean (GPa)		Std dev. (GPa)		Skewness		Kurtosis	
	"True"	Identified	"True"	Identified	"True"	Identified	"True"	Identified
Elasticity								
gPC-EKF	44.95	45.12	10.00	10.54	−0.594	−0.766	2.877	3.703
EKF	44.95	43.85	10.00	2.39	−0.594	–	2.877	–
UKF	44.95	43.55	10.00	2.40	−0.594	–	2.877	–
Poisson's ratio								
gPC-EKF	0.124	0.157	0.068	0.086	0.789	0.707	3.473	3.395
EKF	0.124	0.153	0.068	0.102	0.789	–	3.473	–
UKF	0.124	0.148	0.068	0.103	0.789	–	3.473	–

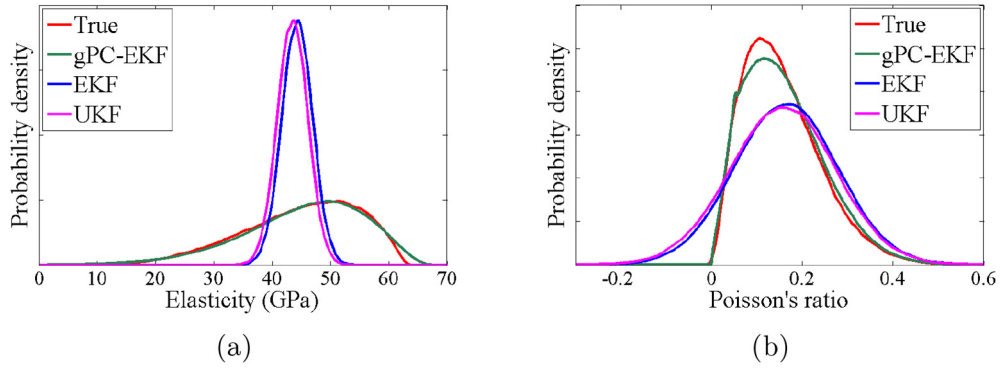

Fig. 4. Performance of proposed gPC-EKF and traditional KF algorithms in identifying "true" densities of system parameters: non-Gaussian case.

3.2. Non-Gaussian case

We continue with the same cantilevered plate, but E and ν are now independent and Beta distributed with parameters listed in Table 7. The first five frequencies are measured 1000 times as before (giving $\overline{\mathbf{Y}}$). Pearson classification scheme classifies each distribution as "three parameter gamma" for which Laguerre polynomials are considered for the gPC expansion. Similar to the Gaussian case, polynomials of order two and three are selected for measurements and system parameters respectively. The Laguerre expansion for the outputs are:

$$\begin{aligned}\widetilde{y}_i(\underline{\xi}) &= y_i(\{\xi_1, \xi_2\}) \\ &= a_0^{y_i} + a_1^{y_i}\xi_2 + a_2^{y_i}\xi_1 + a_3^{y_i}\left(\frac{3}{2}\xi_2^2 - \frac{1}{2}\right) + a_4^{y_i}\xi_1\xi_2 \\ &\quad + a_5^{y_i}\left(\frac{3}{2}\xi_1^2 - \frac{1}{2}\right) \end{aligned} \tag{15}$$

The output gPC coefficients are estimated as before and listed in Table 8. This fitted gPC model for output is employed to simulate a large data set $\widetilde{\mathbf{Y}}$. Table 9 compares the moments of the measured output $\overline{\mathbf{Y}}$ with those of the fitted gPC model $\widetilde{\mathbf{Y}}$.

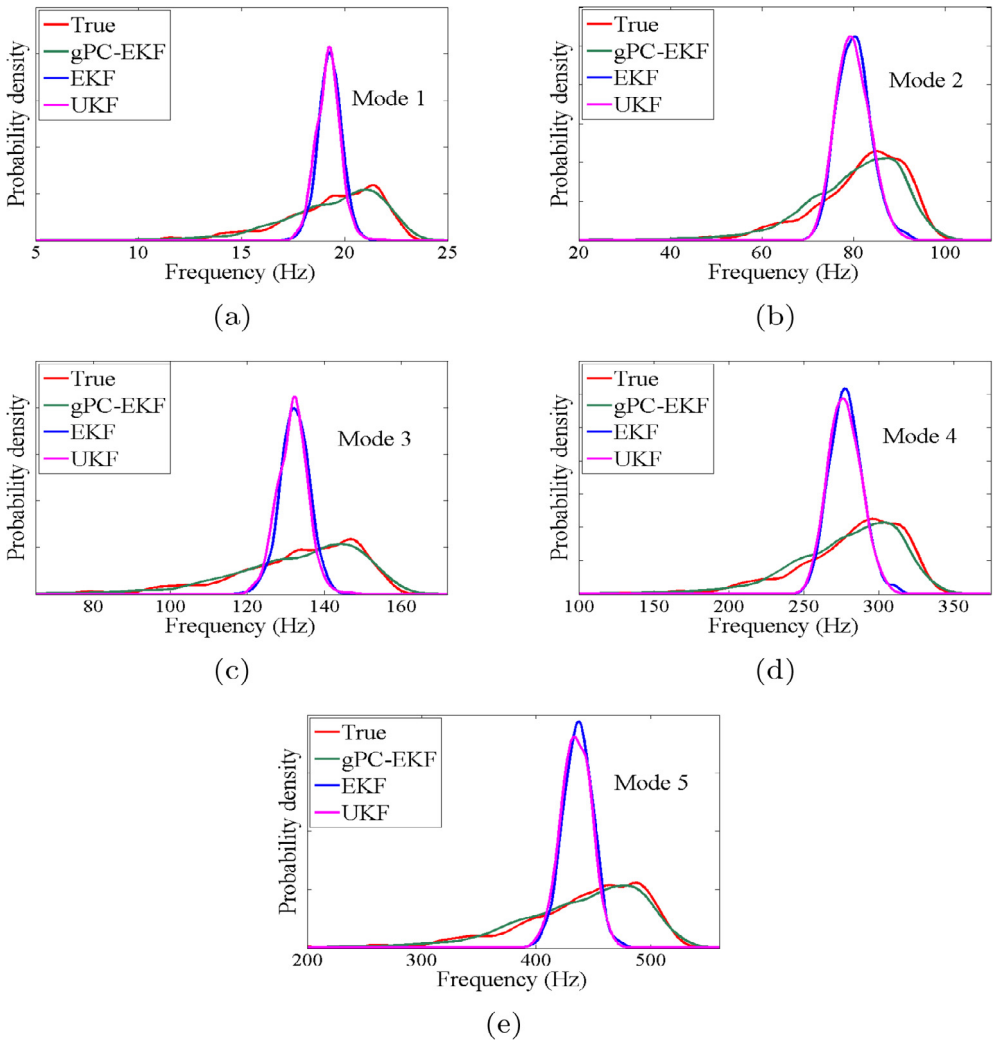

Fig. 5. Performance of proposed gPC-EKF algorithm vis à vis the traditional KF algorithms in reproducing the probability densities of the first five modal frequencies: non-Gaussian system parameters.

Similar to the previous case, the parameter gPC expansion is defined using the same germ set used in Eq. (15):

$$\begin{aligned} x_1(\xi_1) &= a_0^{x_1} + a_1^{x_1}\xi_1 + a_2^{x_1}\left(\frac{3}{2}\xi_1^2 - \frac{1}{2}\right) + a_3^{x_1}\left(\frac{5}{2}\xi_1^3 - \frac{3}{2}\xi_1\right); \\ x_2(\xi_2) &= a_0^{x_2} + a_1^{x_2}\xi_2 + a_2^{x_2}\left(\frac{3}{2}\xi_2^2 - \frac{1}{2}\right) + a_3^{x_2}\left(\frac{5}{2}\xi_2^3 - \frac{3}{2}\xi_2\right); \end{aligned} \tag{16}$$

and proceeding as before with finite element analyses at collocation points and then minimizing the error between the first four moments of $\hat{\mathbf{y}}(\underline{\xi})$ and $\tilde{\mathbf{y}}(\underline{\xi})$, the optimal gPC coefficients are obtained as listed in Table 10.

Fig. 4a and b compares the estimated parameter densities against their "true" densities and Table 11 compares the corresponding moments. Evidently, the proposed method not only identified the mean and standard deviations but also accurately estimated the target distribution by matching up to fourth order moments. Fig. 5 compares the measured *vs.* identified output densities for first five modal frequencies.

As before, we compare the performance of our proposed gPC-EKF technique with those of traditional EKF/UKF techniques. Table 11 demonstrates the inability of EKF and UKF algorithm to correctly identify the parameter probability densities. Fig. 4a and b additionally describe how the forced Gaussian assumption in the EKF/UKF estimation for a non-Gaussian parameter can result in significant errors in the estimates. In contrast, the accuracy of our method is not limited to Gaussian cases; instead, it can identify any arbitrary distribution for which EKF/UKF fails to provide accurate estimates for even the first two moments of the distributions.

4. Conclusion

In this article we coupled Extended Kalman filtering (EKF) with generalized polynomial chaos (gPC) expansion to identify probability distributions of system parameters using the measured output uncertainty. The functional relationship between parameter and output uncertainty is defined using their gPC models. The gPC coefficients for outputs are estimated using Galerkin projection technique while EKF is employed to estimate the same for parameters inversely from the fitted gPC model of the output.

While the traditional Kalman filtering based parameter estimation schemes such as EKF and UKF are limited to Gaussian system parameters, the proposed gPC-EKF approach can estimate arbitrary parameter distributions efficiently and accurately. The numerical study on a system with non-Gaussian parameters demonstrated that with the traditional EKF and UKF algorithms, the forced assumption of Gaussianity causes significant errors in estimation.

In contrast, the proposed gPC-EKF efficiently estimated the arbitrary non-Gaussian parameter distributions matching up to the fourth order moments. The dimensionality of the formulation however increases significantly with the number of parameters and with the order of the polynomial considered. In this formulation dependence between parameters is not considered. Future research will be taken up for systems with correlated parameters. Application of this algorithm in real life problems with strongly nonlinear mechanical systems (e.g., systems with plasticity and/or damage) will also be considered in our future research.

Appendix A

A.1. Pearson classification scheme

This article attempts to identify uncertainty in system parameter from the measured output variability. This necessitates defining the output uncertainty precisely from the measurement before propagating it inversely through the model. In this study the distribution of measured output is defined using Pearson's model criteria [57,58]. Pearson model is a family of continuous distribution defined by the third and fourth order statistics of a dataset. In Pearson model, the density $p(\mathbf{x})$ of a realization $\mathbf{x}$ can be obtained as a solution of this following differential equation:

$$\frac{\partial p(x)}{\partial x} = \frac{\lambda - a - x}{b_2(x-\lambda)^2 + b_1(x-\lambda) + b_0} p(x); \tag{17}$$

where $b_0, b_1, b_2,$ and a are defined as:

$$b_0 = \frac{4\beta_2 - 3\beta_1}{10\beta_2 - 12\beta_1 - 18}\mu_2; \tag{18a}$$

$$a = b_1 = \sqrt{\mu_2}\sqrt{\beta_1}\frac{\beta_2 + 3}{10\beta_2 - 12\beta_1 - 18}; \tag{18b}$$

$$b_2 = \frac{2\beta_2 - 3\beta_1 - 6}{10\beta_2 - 12\beta_1 - 18}; \tag{18c}$$

Skewness β_1 and traditional curtosis β_2 of the measured data set are defined as:

$$\beta_1 = \frac{M_3^2}{\sigma_2^3} \text{ and } \beta_2 = \frac{M_4}{\sigma_2^2}; \tag{19}$$

Depending on different roots of the quadratic denominator function of the right hand side of Eq. (17) Pearson model takes forms of different general distribution type. Thus, using higher order moments Pearson model identifies the best matching distribution type for a given data set.

References

[1] Mockus J. Bayesian Heuristic approach to discrete and global optimization: algorithms, visualization, software, and applications. Springer-Verlag; 2010.
[2] Thompson B, Vladimirov I. Bayesian parameter estimation and prediction in mean reverting stochastic diffusion models. Nonlinear Anal: Theory Methods App 2005;63(5):e2367–75.
[3] Wang J, Zabaras N. Using Bayesian statistics in the estimation of heat source in radiation. Int J Heat Mass Transfer 2005;48(1):15–29.
[4] Khan T, Ramuhalli P. A recursive bayesian estimation method for solving electromagnetic nondestructive evaluation inverse problems. IEEE Trans Magn 2008;44(7):1845–55.
[5] Nocedal J, Wright S. Numerical optimization, series in operations research and financial engineering, Springer, New York, USA.
[6] Floudas CA. Deterministic global optimization, vol. 37. Springer Science & Business Media; 1999.
[7] Horst R. Introduction to global optimization. Springer Science & Business Media; 2000.
[8] Kalman RE et al. A new approach to linear filtering and prediction problems. J Basic Eng 1960;82(1):35–45.
[9] Hoshiya M, Saito E. Structural identification by extended Kalman filter. J Eng Mech 1984;110(12):1757–70.
[10] Maruyama O, Hoshiya M. System identification of an experimental model by extended Kalman filter. New Trends Water Environ Eng Saf Life 2000:181.
[11] Ghanem R, Shinozuka M. Structural-system identification. I: theory. J Eng Mech 1995;121(2):255–64.
[12] Sato T, Takei K. Development of a Kalman filter with fading memory. Proc Struct Saf Reliab 1998. 387-349.
[13] Yoshida I, Damage detection using Monte Carlo filter based on non-Gaussian noise. Structural Safety and Reliability: ICOSSAR'01 (2001); 2001.
[14] Gelb A. Applied optimal estimation. MIT press; 1974.
[15] Welch G, Bishop G, An introduction to the Kalman filter; 1995.
[16] Julier SJ, Uhlmann JK. Unscented filtering and nonlinear estimation. Proc IEEE 2004;92(3):401–22.
[17] Anderson BD, Moore JB. Optimal filtering. Courier Corporation; 2012.
[18] Nasrellah H, Manohar C. Particle filters for structural system identification using multiple test and sensor data: a combined computational and experimental study. Struct Control Health Monit 2011;18(1):99–120.
[19] Radhika B, Manohar C. Updating response sensitivity models of nonlinear vibrating structures using particle filters. Comput Struct 2011;89(11):901–11.
[20] Radhika B, Manohar C. Nonlinear dynamic state estimation in instrumented structures with conditionally linear Gaussian substructures. Probab Eng Mech 2012;30:89–103.
[21] Zghal M, Mevel L, Del Moral P. Modal parameter estimation using interacting Kalman filter. Mech Syst Signal Process 2014;47(1):139–50. Elsevier.
[22] Snyder C, Bengtsson T, Bickel P, Anderson J. Obstacles to high-dimensional particle filtering. Mon Weather Rev 2008;136(12):4629–40.
[23] Evensen G. Sequential data assimilation with a nonlinear quasi-geostrophic model using Monte Carlo methods to forecast error statistics. J Geophys Res: Oceans (1978–2012) 1994;99(C5):10143–62.
[24] Spanos PD, Ghanem R. Stochastic finite element expansion for random media. J Eng Mech 1989;115(5):1035–53.
[25] Wiener N. The homogeneous chaos. Am J Math 1938:897–936.
[26] Ghanem RG, Spanos PD. Spectral stochastic finite-element formulation for reliability analysis. J Eng Mech.
[27] Ghanem R. Ingredients for a general purpose stochastic finite elements implementation. Comput Methods Appl Mech Eng 1999;168(1):19–34.
[28] Karhunen K. Über lineare Methoden in der Wahrscheinlichkeitsrechnung, vol. 37. Universitat Helsinki,; 1947.
[29] Lonvn M, Fonctions aléatoires de second ordre, Supplement to P. Levy, Proces stochastiques et mouvement Brownien. Gauthier-Villars, Paris.
[30] Xiu D, Karniadakis GE. The Wiener-Askey polynomial chaos for stochastic differential equations. SIAM J Sci Comput 2002;24(2):619–44.
[31] Askey R, Wilson JA. Some basic hypergeometric orthogonal polynomials that generalize Jacobi polynomials, vol. 319. American Mathematical Soc.; 1985.
[32] Verlaan M, Heemink A. Nonlinearity in data assimilation applications: a practical method for analysis. Mon Weather Rev 2001;129(6):1578–89.
[33] Xiong X, Navon IM, Uzunoglu B. A note on the particle filter with posterior Gaussian resampling. Tellus A 2006;58(4):456–60.
[34] Xiu D, Karniadakis GE. Modeling uncertainty in steady state diffusion problems via generalized polynomial chaos. Comput Methods Appl Mech Eng 2002;191(43):4927–48.
[35] Xiu D, Karniadakis GE. The Wiener-Askey polynomial chaos for stochastic differential equations. SIAM J Sci Comput 2002;24(2):619–44.
[36] Xiu D, Karniadakis GE. Modeling uncertainty in flow simulations via generalized polynomial chaos. J Comput Phys 2003;187(1):137–67.
[37] Sandu A, Sandu C, Ahmadian M. Modeling multibody systems with uncertainties. Part I: Theor Comput Aspects Multibody Syst Dyn 2006;15(4):369–91.
[38] Sandu C, Sandu A, Ahmadian M. Modeling multibody systems with uncertainties. Part II: Numer App Multibody Syst Dyn 2006;15(3):241–62.
[39] Sandu C, Sandu A, Chan BJ, Ahmadian M. Treating uncertainties in multibody dynamic systems using a polynomial chaos spectral decomposition. In: ASME 2004 International mechanical engineering congress and exposition. American Society of Mechanical Engineers; 2004. p. 821–9.
[40] Blanchard E, Sandu C, Sandu A. A polynomial-chaos-based Bayesian approach for estimating uncertain parameters of mechanical systems. In: ASME 2007 International design engineering technical conferences and computers and information in engineering conference. American Society of Mechanical Engineers; 2007. p. 1041–8.
[41] Soize C, Ghanem R. Physical systems with random uncertainties: chaos representations with arbitrary probability measure. SIAM J Sci Comput 2004;26(2):395–410.
[42] Desceliers C, Ghanem R, Soize C. Maximum likelihood estimation of stochastic chaos representations from experimental data. Int J Numer Methods Eng 2006;66(6):978–1001.
[43] Ghanem RG, Spanos PD. Spanos, Stochastic finite elements: a spectral approach. Courier Corporation; 2003.
[44] Ghanem R, Spanos P. A stochastic finite-element formulation for reliability analysis. Probab Eng Mech 1993;8:255–64.
[45] Sarkar A, Ghanem R. Mid-frequency structural dynamics with parameter uncertainty. Comput Methods Appl Mech Eng 2002;191(47):5499–513.
[46] Witteveen JA, Loeven A, Sarkar S, Bijl H. Probabilistic collocation for period-1 limit cycle oscillations. J Sound Vibr 2008;311(1):421–39.

[47] Kundu A, Adhikari S. Dynamic analysis of stochastic structural systems using frequency adaptive spectral functions. Probab Eng Mech 2015;39:23–38.
[48] Kundu A, Adhikari S. Transient response of structural dynamic systems with parametric uncertainty. J Eng Mech 2013;140(2):315–31.
[49] Schuëller G, Pradlwarter H. Uncertain linear systems in dynamics: retrospective and recent developments by stochastic approaches. Eng Struct 2009;31(11):2507–17.
[50] Sepahvand K, Marburg S, Hardtke H-J. Uncertainty quantification in stochastic systems using polynomial chaos expansion. Int J Appl Mech 2010;2 (02):305–53.
[51] Sepahvand K, Marburg S, Hardtke H-J. Stochastic free vibration of orthotropic plates using generalized polynomial chaos expansion. J Sound Vib 2012;331 (1):167–79.
[52] Blanchard ED, Sandu A, Sandu C. A polynomial chaos-based Kalman filter approach for parameter estimation of mechanical systems. J Dyn Syst Meas Contr 2010;132(6):061404.
[53] Li J, Xiu D. A generalized polynomial chaos based ensemble Kalman filter with high accuracy. J Comput Phys 2009;228(15):5454–69.
[54] Pence BL, Fathy HK, Stein JL. A maximum likelihood approach to recursive polynomial chaos parameter estimation. In: American control conference (ACC), 2010. IEEE; 2010. p. 2144–51.
[55] Pence BL. Recursive parameter estimation using polynomial chaos theory applied to vehicle mass estimation for rough terrain [Ph.D. thesis]. Pennsylvania State University; 2011.
[56] Jacquelin E, Adhikari S, Sinou J-J, Friswell M. Polynomial chaos expansion in structural dynamics: accelerating the convergence of the first two statistical moment sequences. J Sound Vib 2015;356:144–54.
[57] Pearson K. Contributions to the mathematical theory of evolution. II. Skew variation in homogeneous material. Philos Trans R Soc London. A 1895:343–414.
[58] Pearson K. Mathematical contributions to the theory of evolution. X. Supplement to a memoir on skew variation. Philos Trans R Soc London Ser A 1901:443–59.
[59] Li J, Roberts JB. Stochastic structural system identification. Part 1: mean parameter estimation. Comput Mech 1999;24:206–10. Springer.
[60] Li J, Roberts JB. Stochastic structural system identification. Part 2: variance parameter estimation. Comput Mech 1999;24:211–5. Springer.
[61] Wu CL, Ma XP, Fang T. A complementary note on Gegenbauer polynomial approximation for random response problem of stochastic structure. Probab Eng Mech 2006;21:410–9. Elsevier.